Transverse flow effects on high-energy photons emitted by expanding quark-gluon plasma

Jan-e Alam
Variable Energy Cyclotron Centre, 1/AF Bidhan Nagar, Calcutta 700 064, India

D. K. Srivastava
Variable Energy Cyclotron Centre, 1/AF Bidhan Nagar, Calcutta 700 064, India
and Theoretical Physics Institute, University of Minnesota, Minneapolis, Minnesota 55455

Bikash Sinha and D. N. Basu
Variable Energy Cyclotron Centre, 1/AF Bidhan Nagar, Calcutta 700 064, India
(Received 19 February 1993)

High-energy photons emitted in ultrarelativistic nucleus-nucleus collisions at energies reached at the CERN SPS and LHC and the BNL RHIC are discussed as a source of information on the collision dynamics and as a signature of the deconfining phase transition. The energy density and velocity fields of the expanding matter have been computed assuming cylindrical symmetry along the transverse direction and boost invariance along the longitudinal direction. The emission of photons from an expanding quark-gluon plasma undergoing a first-order phase transition has been evaluated. When the transverse flow of the system is accounted for, it is found that the photons having their origin in the hadronic matter are comparable to those originating in the quark-gluon plasma for p_T greater than 2 GeV, at energies reached at the SPS and RHIC. At energies reached at the LHC, photons having a p_T larger than about 4 GeV are shown to have their origin predominantly in the quark-gluon plasma. The location of the p_T window is shown to be very sensitive to the value of the freeze-out temperature chosen. The feasibility of evaluating the direct (QCD) photons has been studied. Photons fragmented off final state quarks in parton-parton scattering are shown to provide the largest background beyond $p_T \approx 3$ GeV at energies reached at the LHC. Accounting for hadronic degrees of freedom beyond the pion is found to be important.

PACS number(s): 25.75.+r, 12.38.Mh, 13.85.Qk, 24.85.+p

I. INTRODUCTION

Quantum chromodynamics (QCD) is firmly established as a viable theory of the strong interaction. One of its most spectacular predictions, a deconfining phase transition from hadronic matter to a quark-gluon plasma (QGP) at high energy densities [1], remains to be verified experimentally. The last decade has witnessed a well-organized international effort by nuclear and high-energy physicists to understand the properties of this exotic state of matter through which the Universe is believed to have passed during its early embryonic period, about a few microseconds after the big bang. On the experimental side, there are efforts to create a "mini bang" in the laboratory by effecting collisions of heavy ions at ultrarelativistic energies at the Super Proton Synchrotron (SPS) and the proposed Large Hadron Collider (LHC) at CERN and the Relativistic Heavy Ion Collider (RHIC) at BNL. At the moment it is believed that in such collisions, energy densities large enough to admit such a phase transition are likely to be achieved, albeit only for a short duration of time.

The QGP created in such collisions is likely to undergo a rapid expansion, which will soon bring down its temperature to the critical value T_C. This will cause a transition back to the hadronic matter which will continue to expand until freeze-out. If the rate of hadronization is not fast enough compared to the cooling rate, we may have additional complexities due to supercooling [2–4] followed by an explosive hadronization. In any case only these hadrons and their decay products are detected, and we look for deviations from "normal collisions" which did not involve a QGP. These so-called "normal collisions" are often simulated by event generators based on string phenomenology [5] or, in recent times, on a judicious combination of string phenomenology (for low transverse momenta) and perturbative QCD to account for "minijets" at larger transverse momenta [6].

For the cleanest signatures to emerge from such interaction, the temperatures attained by the QGP should be as high as possible. However, the higher initial temperatures also imply higher multiplicities and thus larger hadronic densities during the hadronic phase mentioned above. The attendant strong final-state interactions among the hadrons is thus quite likely to wash out some or many of the signatures of the QGP which are based on detection of hadrons. In view of this, it is not surprising that signatures such as the suppression of J/ψ [7], the suppression of anticorrelations [8], and enhancement of strangeness [9] can also be explained, at least to some extent, without invoking any transition to QGP.

It is in this context that photons and dileptons as signatures of the QGP and as probes of the dynamics of the collision [10–21] assume unequivocal importance.

The great advantage of these electromagnetic signals is that since they interact only weakly with the surrounding medium, they have a very large mean free path compared to the size of the system, even during the later stages of the collision. Thus photons and dileptons are *the vehicles for pristine information* about the QGP.

It has been argued that the QGP provides photons mainly through the Compton ($qg \to \gamma q$) and annihilation ($q\bar{q} \to \gamma g$) processes. On the other hand, we have non-QGP photons originating in the early stages of the collision through the hard QCD Compton and annihilation processes (the direct photons), and a substantial background from the decay of π^0 and η mesons. It has been suggested [10–21] that there may be a p_T window spanning the transverse region of about 2–4 GeV where the thermal photons from the QGP may dominate, as the decay photons dominate at lower p_T and the direct (hard QCD) photons at larger p_T.

These arguments have to be refined considerably in order to accommodate the dynamic evolution of the system [22]. Additionally, the onset of photon-emitting hadronic reactions should also be accounted for. Such reactions are facilitated during the mixed and the hadronic phases when the density and the temperature of the hadronic matter are still quite high [21]. A large number of vector mesons created during the hadronization are also likely to decay well before the freeze-out. The hadronic reactions and decay of vector mesons ignored in the past introduce a richness and complexity not envisaged earlier. This aspect finds its best expression in the recent work of Kapusta, Lichard, and Seibert [23] where it is found that "a hadronic gas at a temperature T shines just as brightly as QGP at the same temperature."

We realize, however, that a more direct comparison of the two states of matter as created in a heavy-ion collision should involve a comparison at the same energy or entropy density [24]. Such a comparison must also account for the space-time history of the expanding plasma as pointed out in [23] and first addressed in [24].

Coming back to our discussion about photons, we recall that one of the most promising outcomes of the work of Kapusta, Lichard, and Seibert is that if the dynamics of the collision is dominated by a long-lived mixed phase, then photons provide a very reliable thermometer for the system.

It should also be remembered that, at least in principle, one can identify the photons from the decay of π^0 and η as such [25] from an invariant-mass analysis. However, we are unable to visualize any kinematic scheme at present which can trace the origin of photons to hadronic reactions or to decay of vector mesons in the large multiplicity environment of ultrarelativistic nucleus-nucleus collisions in a reliable manner.

We further realize that the transverse expansion of the plasma becomes important towards the later stages of the dynamics. This can kick photons from the hadronic matter into the p_T window mentioned above and partly disfigure or even obliterate the signature of the QGP photons.

Thus we have to admit that the photons from QGP have only a fighting chance of being discernible if the matter is formed in the mixed phase. However, the hadronic photons will certainly pale beside their counterparts produced in the QGP once the initial temperatures are much larger, say, at LHC.

We would also like to point out that an important input to all the calculations involving integrations over the space-time history of the plasma is the formation time τ_i when the temperature is T_i. Thus the considerations of isentropic longitudinal expansion provide [15] that

$$T_i^3 \tau_i = \frac{2\pi^4}{45\zeta(3)\pi R^2 4 a_Q} \frac{dN}{dy_\pi}, \tag{1}$$

where dN/dy_π is the pion rapidity density, R is the transverse dimension of the system and $a_Q = 37\pi^2/90$ for a system consisting of u and d quarks and gluons. The initial time τ_i is often taken [26] as 1 fm/c. This value is not quite consistent with larger initial temperatures likely to be achieved at RHIC and LHC [20, 21, 27]. The advent of "minijets" at RHIC and LHC energies will enhance $\langle E_T \rangle$ considerably [5] and is likely to lead to a more rapid thermalization. A simple estimate can then be made by noting that the average energy of particles at a temperature T_i is given by $\langle E_T \rangle \simeq 3T_i$. Thus we see that the uncertainty principle would provide for the initial proper time $\tau_i \simeq 1/(3T_i)$.

This would admit much larger initial temperatures [20, 21, 27] than hitherto believed [26] to be achievable at RHIC and LHC for the same multiplicity densities. Fluctuations, if present, may further boost the temperatures. These enhanced temperatures are welcome indeed as they would lead to a copious production of photons from the QGP phase of evolving system.

An additional advantage of these small formation times is that we do not have to worry about the preequilibrium contribution. In this sense our results may also be taken as the physical upper limit for the thermal photons. It may be recalled that parton cascade model calculations provide that most of the entropy in nuclear collisions at LHC and RHIC energies is generated [28] within about 0.1–0.2 fm/c of nuclear contact and a kinetic equilibrium is attained equally rapidly.

Unfortunately, even this blessing in the form of enhanced temperatures is not likely to be without blemish. For example, if the initial temperature $\simeq$ 0.5–1 GeV, there would be a large contribution to the thermal photons from QGP at $p_T \simeq$ 2–4 GeV and its tail may extend at least a few GeV more and into the region we identified earlier for direct QCD photons. It has often been argued that since the direct photons could be described reliably using perturbative QCD, such a description could provide a good normalization for the data.

Thus we see that the task of establishing photons as a signature of QGP even in model calculations is not so easy because we have a multitude of processes leading to the production of photons. In the present work we embark on such a task, and discuss the viability of this exercise by evaluating photons from the life of the plasma up to the freeze-out by accounting for the transverse expansion and comparing it with the direct photons. This corresponds to the ideal situation when the photons from

the decay of π^0 and η mesons after the freeze-out can be identified as such by an invariant-mass analysis. We have adopted this view because the WA 98 group at CERN is in a position to make an accurate distinction [25] for $p_T \geq 1$ GeV and if $\gamma/\pi^0 \geq 0.05$.

It may be remarked that our earlier work in this direction [20, 21, 24] neglected the transverse expansion and that of Ruuskannen [29], considered only the QGP phase.

Yet another important aspect of the present work is a better accounting for the degrees of freedom of the mixed and hadronic phases [20, 21]. This enriched composition is due to the presence of heavier mesons ρ, ω, and η. It has already been noted that this leads to reduced lifetimes for these phases [20, 21, 24] in a purely longitudinal expansion of the plasma. In view of the above we feel that our present work presents a fairly comprehensive, if not exhaustive, perspective for photons as messengers of the advent of QGP.

The paper is organized in the following way. In Sec. II we present results for the direct photons using perturbative QCD. The Compton plus annihilation contributions for a few $p+p$ cases and for a $p+^{12}$C case are compared to the experimental data to demonstrate the reliability of QCD estimates and the feasibility of evaluating the background from QCD photons. Predictions are made for a ^{208}Pb+^{208}Pb collision reached at the SPS, RHIC, and LHC, along with the direct photons radiated off the final-state quark. In Sec. III we detail the hydrodynamic treatment used to describe the expansion and cooling of the thermalized plasma. In Sec. IV we present results of our estimates for photons as signatures of QGP. A summary is given in Sec. V.

II. DIRECT PHOTONS

A powerful and classic test of QCD in hard collisions is provided by measurements of direct photons proceeding via the subprocesses

$$q(\bar{q}) + g \rightarrow \gamma + q(\bar{q}), \tag{2}$$

$$q + \bar{q} \rightarrow \gamma + g. \tag{3}$$

These subprocesses (Fig. 1) are fairly well understood both experimentally [30] and theoretically [31]. It has often been suggested that one may use these predictions to obtain normalizations for the data at larger transverse momenta. The cross section in the leading order of perturbative QCD is easily obtained by convoluting the cross section for the elementary process with the gluon or quark contents of the participating hadrons. Thus we have

$$E_\gamma \frac{d\sigma}{d^3p_\gamma}(A+B \rightarrow \gamma + \cdots) = \int \frac{dx_a\,dx_b}{x_a x_b} F(a,A;x_a) F(b,B;x_b) E_\gamma \frac{d\hat{\sigma}}{d^3p_\gamma}, \tag{4}$$

where the invariant cross section for the subprocess

$$a + b \rightarrow c + \gamma \tag{5}$$

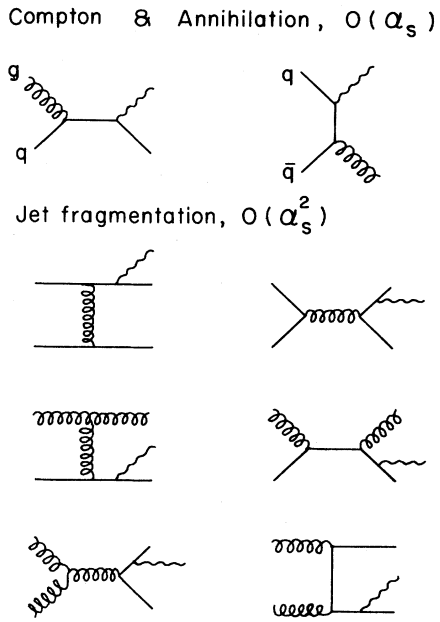

FIG. 1. Compton and annihilation graphs for emission of photons and graphs leading to a photon fragmented off a final-state quark.

is written as

$$E_\gamma \frac{d\hat{\sigma}}{d^3p_\gamma} = \frac{\hat{s}}{\pi}\frac{d\sigma}{d\hat{t}}\delta(\hat{s}+\hat{t}+\hat{u}), \tag{6}$$

where $\hat{s}$, $\hat{t}$, and $\hat{u}$ are the Mandelstam variables for the subprocess (5). For the detection of photons emitted at 90°, so that their rapidity is zero, we have

$$\hat{s} = x_a\, x_b\, s, \tag{7}$$

$$\hat{u} = -\,x_b\, x_T\, s/2, \tag{8}$$

$$\hat{t} = -\,x_a\, x_T s/2, \tag{9}$$

$$x_T = \frac{2p_T}{\sqrt{s}}. \tag{10}$$

Here s is the square of the total energy in the center-of-mass system and p_T is the transverse momentum of the photon. We have assumed that the partons have a vanishing mass and the F's give us the probability of finding partons with momentum fractions x_i.

The elementary cross sections for the leading $[O(\alpha_s)]$ subprocesses (2) and (3) are [32–34],

$$\frac{d\sigma}{d\hat{t}}(qg \rightarrow q\gamma) = -\frac{\pi\alpha\alpha_s}{3\hat{s}^2} e_q^2 \frac{\hat{u}^2+\hat{s}^2}{\hat{u}\hat{s}} \tag{11}$$

and

$$\frac{d\sigma}{d\hat{t}}(\bar{q}q \rightarrow g\gamma) = \frac{8\pi\alpha\alpha_s}{9\hat{s}^2} e_q^2 \frac{\hat{u}^2+\hat{t}^2}{\hat{u}\hat{t}}, \tag{12}$$

where e_q is the charge of the interacting quark. These expressions are easily simplified to yield the contribution of the Compton graph:

$$\frac{d\sigma^C(y=0)}{dy\,d^2p_T} = \frac{\alpha\alpha_s}{3s^2(x_T/2)}\int_{x_{\min}}^1 \frac{dx_a}{x_a-(x_T/2)}\left[F_2(x_a;A)G(x_b;B)\frac{x_b^2+(x_T/2)^2}{x_a^2x_b^3}+(x_a\leftrightarrow x_b;A\leftrightarrow B)\right], \tag{13}$$

where

$$x_b = \frac{x_a x_T}{2x_a - x_T},\quad x_{\min} = \frac{x_T}{2-x_T} \tag{14}$$

and

$$F_2(x) = x\sum e_q^2\,[q(x)+\bar{q}(x)],\quad G(x) = xg(x). \tag{15}$$

Similarly, the result for the annihilation graph is given by

$$\frac{d\sigma^A(y=0)}{dy\,d^2p_T} = \frac{8\alpha\alpha_s}{9s^2}\int_{x_{\min}}^1 \frac{dx_a}{x_a-(x_T/2)}\left[Q_2(x_a;A)\bar{Q}(x_b;B)\frac{x_a^2+x_b^2}{x_a^3x_b^3}+(x_a\leftrightarrow x_b;A\leftrightarrow B)\right], \tag{16}$$

where we have defined

$$Q_2(x) = x\sum e_q^2 q(x), \bar{Q}(x) = x\sum \bar{q}(x). \tag{17}$$

The strong "running coupling constant" is given by [32,33],

$$\alpha_s(Q^2) = \frac{12\pi}{(33-2N_f)\ln(Q^2/\Lambda^2)}, \tag{18}$$

where N_f is the number of flavors and Λ is the QCD scale parameter. Following Aurenche *et al.* [35] we have taken the number of flavors as four and $\Lambda = 0.2$ GeV, and chosen $Q^2 = p_T^2$ for the evaluation of direct photons.

It is expected that at higher incident energies corrections to the Compton and annihilation graphs should become important. This bremsstrahlung process, where a photon is radiated off the final-state quark in a $2\to 2$ jet event, can be visualized as an $O(\alpha_s^2)$ correction (Fig. 1).

The photon couples to the charge of the quark and the resulting fragmentation function to the leading-logarithmic approximation is [31]

$$zD_{q\to\gamma}(z,Q^2) = e_q^2\frac{\alpha}{2\pi}[1+(1-z)^2]\ln(Q^2/\Lambda^2) \tag{19}$$

and

$$zD_{g\to\gamma}(z,Q^2) = 0, \tag{20}$$

where z represents the fraction of the jet momentum carried by the (collinear) photon. We quote only the final result [15] for the bremsstrahlung contribution by using the method of effective structure function:

$$\frac{d\sigma^B(y=0)}{dy\,d^2p_T} = K\frac{\alpha\alpha_s^2}{2\pi s^2}\ln\frac{p_T^2}{\Lambda^2}\frac{1}{x_T}\int_{x_T}^1 dy_T\frac{1}{(y_T/2)^2}\left[1+(1-x_T/y_T)^2\right]$$
$$\times\int_{y_T/(2-y_T)}^1\frac{dx_a}{x_a-y_T/2}\times\left[F_2(x_a;A)\left(G(x_b;B)+\frac{4}{9}Q(x_b;B)\right)\frac{x_a^2+(y_T/2)^2}{x_a^4}\right.$$
$$\left.+(x_a\leftrightarrow x_b;A\leftrightarrow B)\right], \tag{21}$$

where

$$x_b = \frac{x_a y_T}{2x_a - y_T} \tag{22}$$

and

$$Q(x) = x\sum[q(x)+\bar{q}(x)]. \tag{23}$$

We have included a normalization factor $K\approx 2$ to account for higher-order corrections which are necessary to adequately reproduce the two jet cross sections [36]. It should also be kept in mind that, because of the logarithmic term in Eq. (21), the bremsstrahlung contribution is also effectively of order α_s. We shall see that this plays a crucial role in enhancing its importance.

In Fig. 2 we show the predictions for the Compton contribution along with the annihilation term for $p+p\to\gamma+X$ experiments at two typical energies reached at the CERN Intersecting Storage Rings (ISR). The experimental data are from Ref. [37] and the structure functions correspond to Duke and Owens, set I [38].

It is seen that the annihilation contribution is small for such pp collisions and that the $O(\alpha_s)$ contributions reproduce the data well enough for the purposes of the present work without any free parameter. Higher-order corrections $O(\alpha_s^2)$ are known to reproduce these data quite accurately [35] and thus we have not shown them separately in this figure.

In Fig. 3 we show our results for $p+^{12}$C [39] at SPS energy and for $p+p$ [40] at a similar energy. We see again that the Compton term dominates and that the leading-

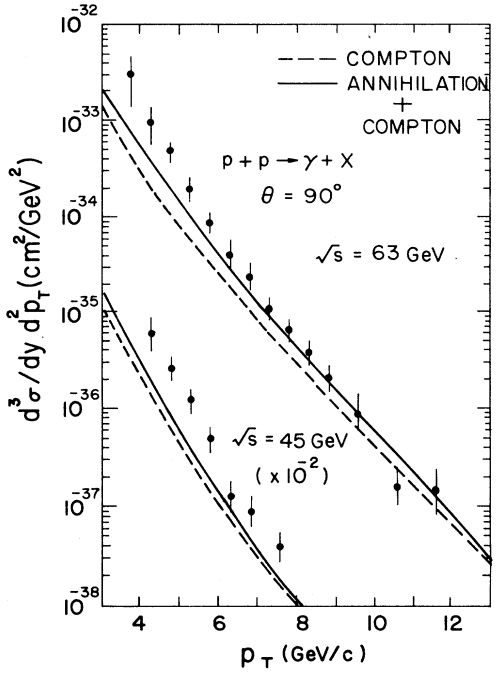

FIG. 2. Compton and Compton + annihilation contributions to direct QCD photons at ISR energies for $p+p$ collision. The experimental data are from Anassontriz *et al.* [37] and the structure functions are from the parametrizations of Duke and Owens, set I [38].

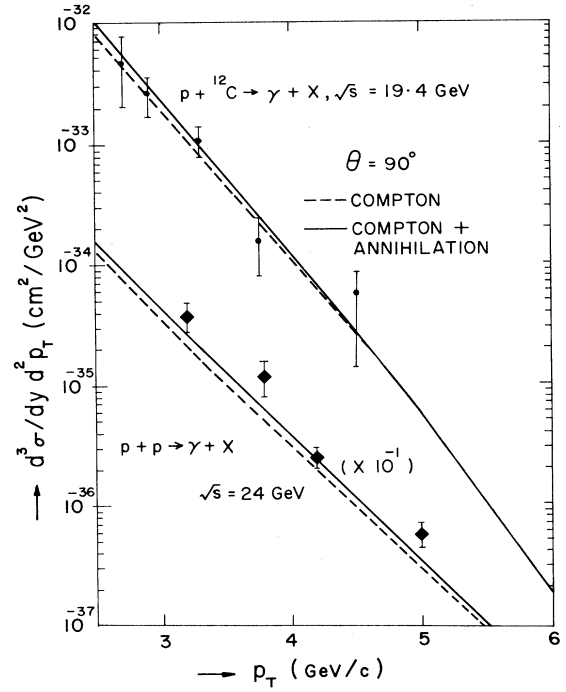

FIG. 3. Compton and Compton + annihilation contributions to direct QCD photons at SPS energies for $p + p$ and $p+^{12}$C collisions. The experimental data are from [39, 40] and the structure functions are from the parametrizations of Duke and Owens, set I [38].

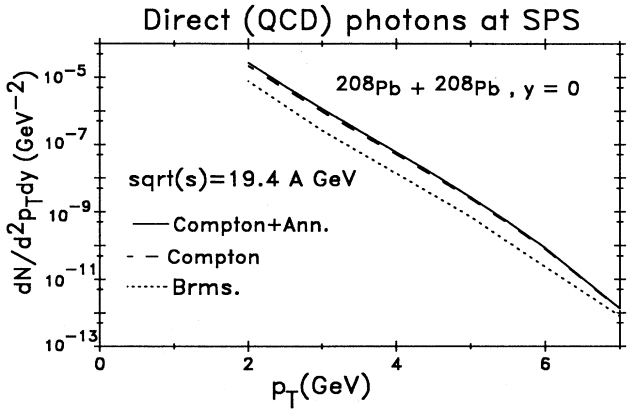

FIG. 4. The Compton, Compton + annihilation, and jet fragmentation contributions to direct photons at SPS energies at central rapidity for ^{208}Pb+^{208}Pb collisions. The structure functions are from Duke and Owens, set I [38]. The fragmentation contribution is seen to be small.

order $O(\alpha_s)$ calculations are able to reproduce the data fairly accurately without any adjustable parameters.

Thus these results hold out the promise that it should be possible to predict the production of direct photons to a good accuracy using the methods of perturbative QCD and including only the leading terms, at and around SPS energies. As stated earlier, the treatment given here is known to reproduce the jet fragmentation cross sections in $p + p$ collisions quite accurately [36].

In Figs. 4–6 we give the results for such an exercise for the collision of lead nuclei at SPS, RHIC, and LHC energies. We have ignored the modification of the structure functions due to the European Muon Colloboration (EMC) effect (and parton shadowing) to avoid introduction of any uncertainty due to specific parametrizations.

We find interesting results. At all the energies the annihilation process gives only a negligible contribution.

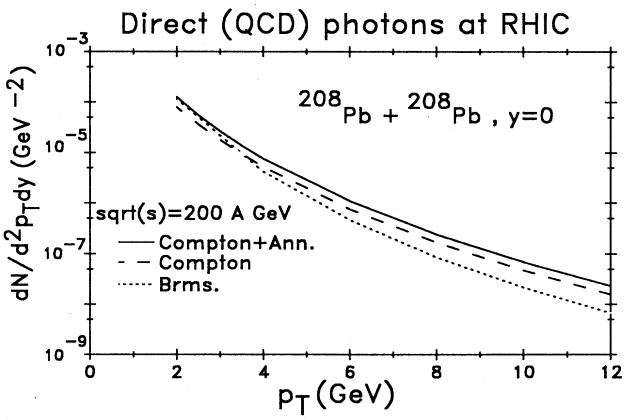

FIG. 5. Compton, Compton + annihilation, and jet fragmentation contributions to direct photons at RHIC energies at central rapidity for ^{208}Pb+^{208}Pb collisions. The structure functions are from Duke and Owens, set I [38]. The fragmentation contribution is seen to be comparable to the Compton process at smaller p_T.

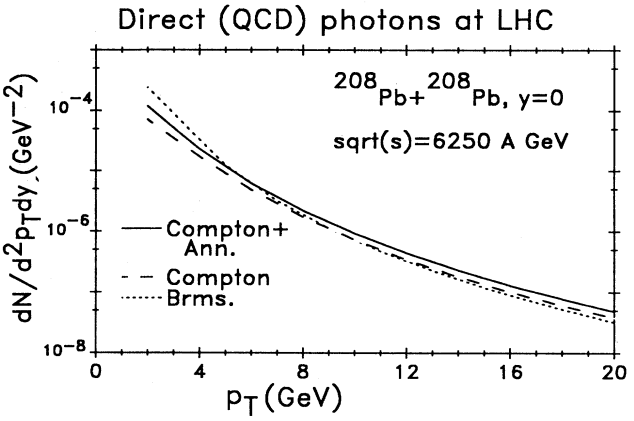

FIG. 6. Compton, Compton + annihilation, and jet fragmentation contributions to direct photons at LHC energies at central rapidity for ^{208}Pb+^{208}Pb collisions. The structure functions are from Duke and Owens, set I [38]. The fragmentation contribution is seen to provide the largest QCD background at smaller p_T.

However, the fragmentation processes (bremsstrahlung) which give only a small contribution at SPS energies become comparable to the Compton processes at RHIC energies. Their contribution is even larger than that for the $O(\alpha_s)$ processes at LHC energies in the interesting range of p_T ≈2–4 GeV, which is the window we shall be concentrating on while looking for the signature of QGP. Considering that decay photons are not likely to populate the large-p_T region, our results indicate that bremsstrahlung photons could be the largest non-QGP background at LHC energies (see Sec. V).

This calls for a quantitative understanding of direct photons which would then provide a convenient and reliable vista for an exciting forage into the realm of QGP.

III. HYDRODYNAMIC FLOW

We have already mentioned that if the energy density achieved during ultrarelativistic collision of nuclei is large enough we may have a transition to QGP. This matter, once created, will undergo a rapid expansion due to internal pressure which will lead to cooling. A pure longitudinal expansion according to the boost-invariant hydrodynamics of Bjorken [41] represents a very useful first approximation. Yet after a time $\tau \approx R/c_s$, where R is the transverse dimension of the system and c_s is the velocity of sound, the rarefaction wave front is likely to reach the center of the expanding system and then we cannot ignore the transverse expansion. The most obvious outcome of this flow is to impart an additional transverse (collective) momentum to the particles and their reaction products. It also leads to a more rapid cooling of the system and a reduced lifetime for the interacting plasma.

These aspects have been discussed in some detail [22, 42–44], and we shall apply the techniques developed there with a more realistic accounting of the degrees of freedom for the hadronic matter and for temperatures likely to be attained at SPS, RHIC, and LHC energies.

One may question the use of hydrodynamics until it is explicitly established that thermalization has been achieved by the time τ_i. We have already stated that the onset of the "minijet" phenomenon at the RHIC and LHC energies will considerably enhance the transverse energy and hence the likely temperature of the plasma. Shuryak [45] has demonstrated that the relaxation time for gluons is $\tau_g \approx 1/(30\alpha_s^2 T)$ and hence they should be thermalized rapidly with an increase in temperature. [By the way this estimate is very close to $\tau_i \approx 1/(3T_i)$ given above for reasonable values of α_s.]

The authors of Ref. [27] have compared results for the emission of dileptons in two extreme scenarios: first, a thermalized hydrodynamically expanding plasma and, second, a free-streaming noninteracting gas of quarks and gluons. The results are not very different from each other. There is no reason to believe that the same should not hold for the emission of photons. Thus it is felt that a more rigorous treatment which may lie somewhere between these two extremes should not greatly alter our findings. The same cannot be said if the phase transition is *not* first order or when the hadronization is *not* fast enough to avoid supercooling [2, 3]. We postpone discussion of these aspects to a future publication.

A. Equation of state

To deal with hydrodynamic flow we have to define an equation of state for the QGP, the mixed, and the hadronic phases. We take the bag model equation of state for the QGP phase and write

$$P_Q(T) = g_Q \frac{\pi^2}{90} T^4 - B, \tag{24}$$

where

$$g_Q = 2 \times 8 + 2 \times 2 \times 2 \times 3 \times \tfrac{7}{8} \tag{25}$$

for a quark matter consisting of massless u and d quarks, gluons, and B is the bag constant.

For the hadronic matter we write

$$P_H(T) = g_H \frac{\pi^2}{90} T^4 \tag{26}$$

and note that for a massless pionic gas $g_H = g_\pi = 3$. However, we have already noted [20, 21, 24] that it is not quite proper to treat the hadronic matter as a dilute gas consisting of only (massless) pions in view of the high temperatures which are likely to be encountered during the hadronization at the critical temperature ($T \approx 200$ MeV) and up to the time of freeze-out ($T \approx 100$ MeV). In order to utilize the simplicity of the relation (26) we replace g_H by $g_{\rm eff}$ with the provision that the entropy density s_H for the hadronic matter can be written as

$$\begin{aligned} s_H &= (\epsilon_H + P_H)/T \\ &= 4 g_{\rm eff} \frac{\pi^2}{90} T^3, \end{aligned} \tag{27}$$

where

$$\epsilon_H = \sum_i g_i \int \frac{\sqrt{p^2+m_i^2}}{\exp[\sqrt{p^2+m_i^2}/T]-1}\frac{d^3p}{(2\pi)^3} \tag{28}$$

and

$$P_H = \sum_i g_i \int \frac{p^2}{3(p^2+m_i^2)^{1/2}}\frac{1}{\exp[\sqrt{p^2+m_i^2}/T]-1} \times \frac{d^3p}{(2\pi)^3}. \tag{29}$$

We take the hadronic gas as consisting of π, ρ, ω, and η mesons with the appropriate statistical factors (g_i) and masses (m_i). Now the speed of sound, c_s, for the hadronic matter is obtained as

$$c_s^{-2} = \frac{T}{s}\frac{ds}{dT} = \left[\frac{1}{g_{\rm eff}(T)}\frac{dg_{\rm eff}(T)}{dT}T+3\right]. \tag{30}$$

We find that $c_s^2 \approx 0.238$ for the situation discussed here, which is somewhat smaller than the value 1/3 which one gets for the case of massless pions.

It is important to realize that the lifetimes of the mixed and the hadronic phases get much shorter when the hadronic matter has a richer constitution compared to the situation when it consists of only pions. This is easily seen by noting that for our case $g_{\rm eff} \approx 4.59$, and hence *if there is only a longitudinal expansion of the plasma*, the end of the QGP phase will occur at the proper time τ_Q:

$$\tau_Q = \left[\frac{T_i}{T_C}\right]^3 \tau_i, \tag{31}$$

where τ_i and T_i are the initial time and the initial temperature. The end of the mixed phase will occur at the proper time

$$\tau_H = \left[\frac{g_Q}{g_{\rm eff}}\right]\tau_Q \tag{32}$$

and the freeze-out will take place at

$$\tau_F = \left[\frac{T_C}{T_F}\right]^3 \tau_H, \tag{33}$$

implying a decrease by a factor $\approx g_{\rm eff}/g_\pi \approx 1.5$ in the lifetimes of the mixed phase and the hadronic phase compared to the scenario when the hadronic matter consists of only pions. It has been noted recently [21] that this results in enhancing the electromagnetic signal from the QGP relative to the background from the hadronic matter by suppressing the latter contribution. The situation is likely to get more complex with the inclusion of transverse flow.

In what follows we shall take $T_C = 160$ MeV and fix $T_F = 100$ MeV. Thus the bag constant B is now obtained as

$$B = (g_Q - g_{\rm eff})\frac{\pi^2}{90}T_C^4. \tag{34}$$

It is noted immediately that for a given bag constant a change in the constitution of the hadronic matter would imply a change in the critical temperature and also a change in the lifetime of the QGP phase through Eq. (31). However, we find [24] that the change in T_C for a given B due to the change in the composition of the hadronic matter as envisaged here is only a few percent. Thus the richness of the hadronic matter considered here does not change the lifetime of the QGP to any significant extent. We shall therefore fix T_C at 160 MeV as mentioned before irrespective of the composition of the hadronic matter.

With these considerations we find that the energy density of the quark matter at the critical temperature is

$$\epsilon_Q(T_C) = 1.34 \ \ {\rm GeV/fm^3}. \tag{35}$$

For the hadronic matter consisting of π, ρ, ω, and η mesons the energy densities at T_C and T_F are given by

$$\epsilon_H(T_C) = 0.18 \ \ {\rm GeV/fm^3}, \tag{36}$$

$$\epsilon_H(T_F) = 0.016 \ \ {\rm GeV/fm^3}. \tag{37}$$

If the hadronic matter is assumed to consist of *only pions*, we have, correspondingly,

$$\epsilon_Q(T_C) = 1.36 \ \ {\rm GeV/fm^3}, \tag{38}$$

$$\epsilon_H(T_C) = 0.084 \ \ {\rm GeV/fm^3}, \tag{39}$$

$$\epsilon_H(T_F) = 0.013 \ \ {\rm GeV/fm^3}. \tag{40}$$

B. Transverse flow at SPS, RHIC, and LHC

We briefly recall the relevant hydrodynamic equations for the sake of completeness. The local energy-momentum conservation is described by the equation

$$\partial_\mu T^{\mu\nu} = 0. \tag{41}$$

Treating the matter produced in the collisions as an ideal fluid, the energy-momentum tensor is given by

$$T^{\mu\nu} = (\epsilon + P)u^\mu u^\nu + g^{\mu\nu}P, \tag{42}$$

where ϵ is the energy density, P is the pressure, and u^μ is the four-velocity of the collective flow:

$$u^\mu = (\gamma, \gamma\mathbf{v}), \tag{43}$$

where $\gamma = 1/\sqrt{1-v^2}$ and $g^{\mu\nu}$ is the metric tensor. We neglect the viscous drag, and thus the expansion is isentropic, which leads to

$$\partial_\mu s^\mu = 0, \tag{44}$$

$$s^\mu = s u^\mu, \tag{45}$$

where s is the entropy density. In the treatment to follow we shall take the net baryon density to be negligible and thus the temperature of the fluid remains the only independent thermodynamic variable. This should be a good approximation insofar as the net baryon density divided

by the total entropy remains small, which is expected to be valid for the ultrarelativistic energies involving heavy nuclei. We shall further assume that the longitudinal flow has a scaling solution. Then boost invariance along the longitudinal direction, together with $u^\mu u_\mu = -1$, requires that the fluid four-velocity for cylindrical symmetry be of the form

$$u^\mu = \gamma_r(\tau, r)(t/\tau, v_r \cos\phi, v_r \sin\phi, z/\tau), \tag{46}$$

where we have used

$$\gamma_r = [1 - v_r^2(\tau, r)]^{-1/2}, \tag{47}$$

$$\tau = (t^2 - z^2)^{1/2}, \tag{48}$$

$$\eta = \frac{1}{2} \ln \frac{t+z}{t-z}. \tag{49}$$

Thus all the Lorentz scalars are functions of τ and r only, and independent of η. Now the hydrodynamic equations of motion for a $(3+1)$-dimensional expansion with cylindrical symmetry and boost invariance along the longitudinal direction read [42]

$$\partial_\tau T^{00} + r^{-1}\partial_r(rT^{01}) + \tau^{-1}(T^{00} + P) = 0, \tag{50}$$

$$\partial_\tau T^{01} + r^{-1}\partial_r[r(T^{00} + P)v_r^2] + \tau^{-1}T^{01} + \partial_r P = 0, \tag{51}$$

with

$$T^{00} = (\epsilon + P)u^0 u^0 - P \tag{52}$$

and

$$T^{01} = (\epsilon + P)u^0 u^1. \tag{53}$$

These equations are solved for the equation of state discussed earlier for times $\tau > \tau_i$ using the relativistic version of the flux-corrected transport algorithm [46]. The initial conditions are chosen such that $v_r(\tau_i, r) = 0$ along with a given initial energy density $\epsilon(\tau_i, r) = \epsilon_i$ within the transverse radius R.

To make our discussion more specific we shall consider central collisions of ^{208}Pb+^{208}Pb at the SPS, RHIC, and LHC energies which correspond to about 20 GeV/A, 200 GeV/A, and 6250 GeV/A, respectively, in the center-of-mass system. The particle rapidity density in the central region is taken as 624, 1735, and 5624, respectively, at the three energies based on considerations detailed in Ref. [27]. The initial temperature is estimated by assuming [21, 27] that $\tau_i \simeq 1/3T_i$ along with Eq. (1). This leads to a temperature of 320 MeV at SPS, 532 MeV at RHIC, and 958 MeV at LHC for a QGP consisting of u and d quarks and gluons.

Hydrodynamic flows for these combinations of initial temperature and time were evaluated using the method of [42]. We would like to recall the important observation of [22] which provides that the results for the hydrodynamic flow obtained below will alter only slightly if some other combination of initial temperature and inital time satisfying (1) is chosen. However, the emissions from the QGP phase would be altered strongly as higher initial temperatures imply larger emissions from this phase.

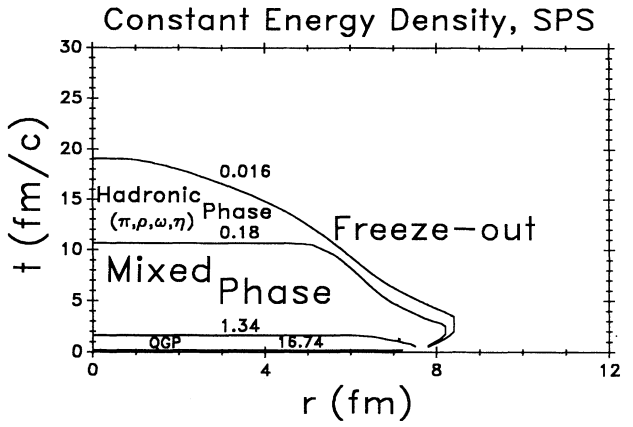

FIG. 7. Energy density (in GeV/fm^3) contours at SPS energies defining the space-time boundaries of the QGP phase, the mixed phase, the hadronic phase, and the freeze-out at $z = 0$. The hadronic matter is composed of π, ρ, ω, and η mesons. The initial temperature $T_i = 320$ MeV and the initial time $\tau_i = 0.206$ fm/c, corresponding to the pion rapidity density $dN/dy_\pi = 624$. The transition temperature T_C is taken as 160 MeV, and the freeze-out is assumed to take place at $T_F = 100$ MeV. The QGP is assumed to consist of u and d quarks and gluons.

We present some of the results in the following.

For SPS energies (Fig. 7) when we choose $T_i = 320$ MeV, $\tau_i = 0.206$ fm/c, and take the hadronic matter to be consisting of π, ρ, ω, and η mesons we see that the QGP phase does not experience any transverse flow and even during the mixed phase only the fluid elements at larger transverse radii experience transverse motion. Thus the dynamics of the plasma at SPS energies

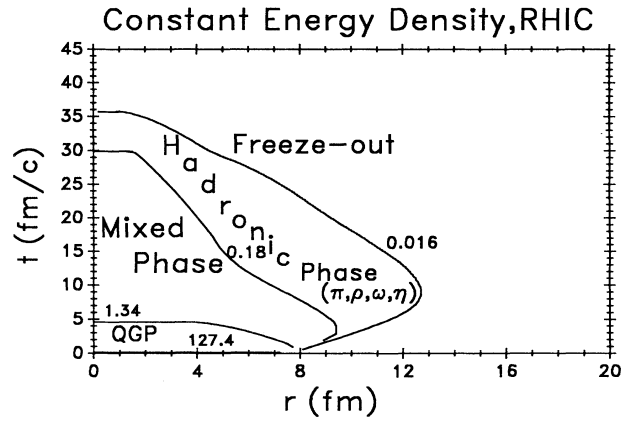

FIG. 8. Energy density (in GeV/fm^3) contours at RHIC energies defining the space-time boundaries of the QGP phase, the mixed phase, the hadronic phase, and the freeze-out at $z = 0$. The hadronic matter is composed of π, ρ, ω, and η mesons. The initial temperature $T_i = 532$ MeV and the initial time $\tau_i = 0.124$ fm/c, corresponding to the pion rapidity density $dN/dy_\pi = 1735$. The transition temperature T_C is taken as 160 MeV, and the freeze-out is assumed to take place at $T_F = 100$ MeV. The QGP is assumed to consist of u and d quarks and gluons.

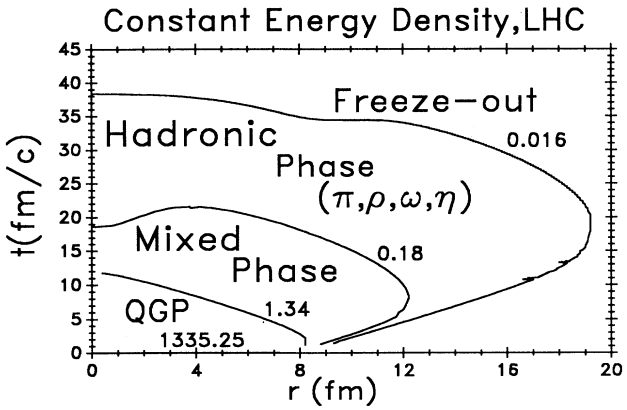

FIG. 9. Energy density (in GeV/fm^3) contours at LHC energies defining the space-time boundaries of the QGP phase, the mixed phase, the hadronic phase, and the freeze-out at $z = 0$. The hadronic matter is composed of π, ρ, ω, and η mesons. The initial temperature $T_i = 958$ MeV and the initial time $\tau_i = 0.069$ fm/c, corresponding to the pion rapidity density $dN/dy_\pi = 5624$. The transition temperature T_C is taken as 160 MeV, and the freeze-out is assumed to take place at $T_F = 100$ MeV. The QGP is assumed to consist of u and d quarks and gluons.

is characterized by a short-lived longitudinally expanding QGP phase, a long-lived mixed phase undergoing a marginal transverse expansion at the edges, and a long-lived hadronic phase undergoing a fairly rapid transverse expansion.

For RHIC energies (Fig. 8) we choose $T_i = 532$ MeV, $\tau_i = 0.1236$ fm/c. We note that the fluid elements at larger transverse radii in the QGP phase itself are affected by the transverse expansion and a large part of the fluid is in transverse motion by the end of the mixed phase. By the time freeze-out occurs the transverse dimension of the system is almost doubled. Curiously enough, this also reduces the lifetime of the hadronic phase at the center. Thus the dynamics of the plasma at RHIC energies is likely to be dominated by a somewhat longer-living QGP phase and a very-long-lived mixed

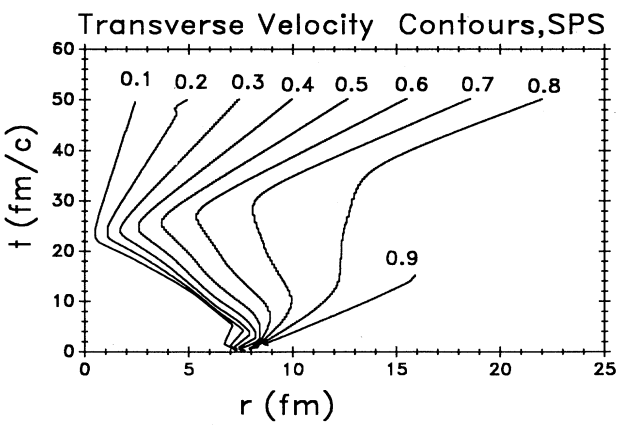

FIG. 10. Transverse velocity contours at SPS energies at $z = 0$ corresponding to the conditions in Fig. 7.

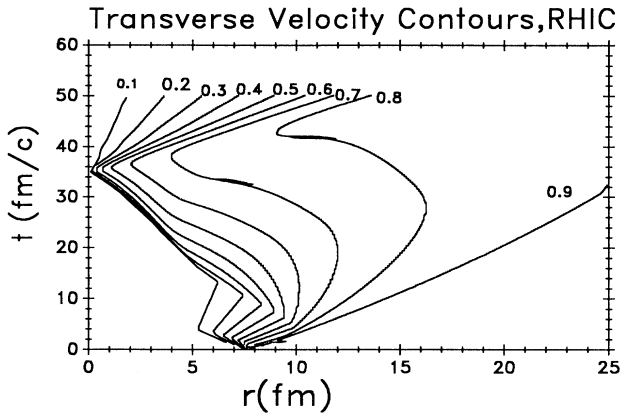

FIG. 11. Transverse velocity contours at RHIC energies at $z = 0$ corresponding to the conditions in Fig. 8.

phase, a part of which is in rapid transverse motion.

The scenario at LHC energies (Fig. 9), where we have $T_i = 958$ MeV and $\tau_i = 0.069$ fm/c, is very interesting indeed as the entire fluid is in transverse motion in the QGP phase itself (recall $R/c_s \approx 12$ fm/c). This has the interesting consequence of suppressing the mixed phase. However, by the time freeze-out occurs the system has almost tripled its transverse dimension.

Thus the dynamics of the plasma at LHC energies is dominated by a long-lived (and also very hot) QGP phase and a cold but rapidly expanding hadronic phase. It is this feature which we feel makes the LHC energies most suitable for a search for a QGP if we can find a reliable method to delineate the transverse expansion effects.

Contours for the transverse velocities for the three energies are given in Figs. 10–12. We note that the phase transition introduces remarkable features into the velocity distributions which may not be easily parametrized in any simple form. We again note that at late times, at least near the edges, the transverse velocities are very high.

In order to illustrate the importance of the heavier mesons in the hadronic matter, we show the energy-

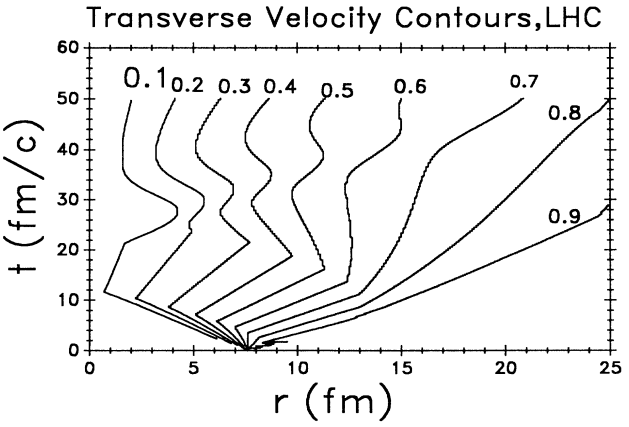

FIG. 12. Transverse velocity contours at LHC energies at $z = 0$ corresponding to the conditions in Fig. 9.

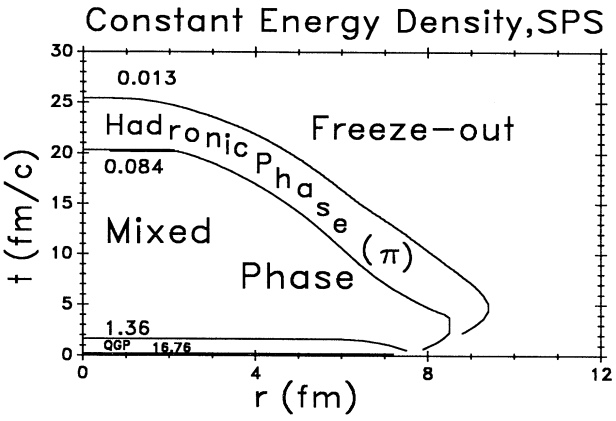

FIG. 13. Same as Fig. 7 (at SPS energies) except that the hadronic matter is assumed to consist of massless π mesons only.

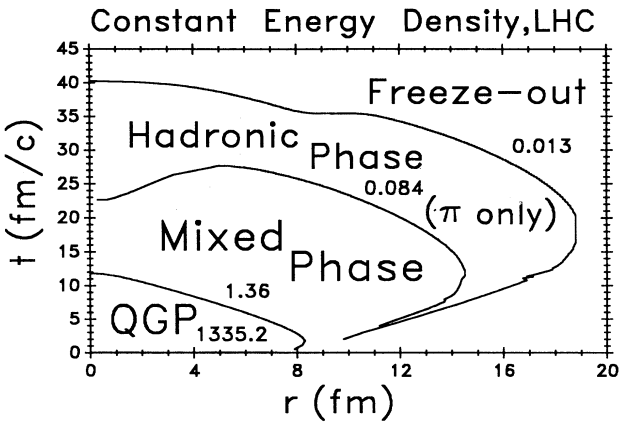

FIG. 15. Same as Fig. 9 (at LHC energies) except that the hadronic matter is assumed to consist of massless π mesons only.

density contours for the three beam energies in Figs. 13–15 for the situation when the hadronic matter is assumed to consist of only massless pions. A comparison of these results with the corresponding results in Figs. 7–9 reveals that with the introduction of heavier mesons, the four-volume available for the mixed phase is decreased substantially. This also limits the time available for the transverse flow to develop. This would definitely help to strengthen the signals from the QGP in comparison to those from the mixed phase and hadronic matter.

We should also remember the following remarkable features introduced by the transverse flow. In the absence of transverse flow, the lifetimes of the mixed phase and the hadronic phase are rather large [Eqs. (32) and (33)]. The transverse flow decreases the lifetime, but increases the spatial dimensions of the system. Thus the overall four-volume of the system is not altered very substantially. Again, the more rapid cooling introduced by the transverse expansion would reduce the emission of photons having larger transverse momenta. However, the photons will now be Doppler shifted and will appear with an enhanced p_T due to transverse flow, thus mimicking emissions from a source having a larger temperature. We shall see later that if the temperature of the source is known this aspect can be used to get a direct and reliable estimate of the "transverse kick" received by the photons.

We have already noted that the transverse flow affects the mixed and the hadronic phases most strongly. In view of the above, this does not augur well for the p_T window for thermal photons [20, 21] from the QGP, unless the initial temperatures are quite high. We shall see in the next section that this is indeed the case.

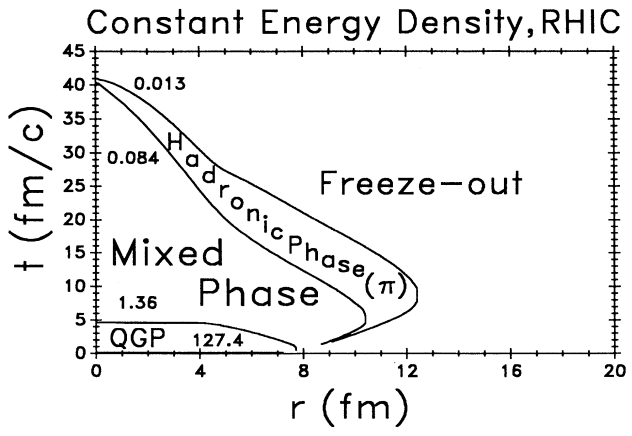

FIG. 14. Same as Fig. 8 (at RHIC energies) except that the hadronic matter is assumed to consist of massless π mesons only.

IV. THERMAL PHOTONS AT SPS, RHIC, AND LHC

We have noted earlier the important finding of Kapusta, Lichard, and Seibert [23] that the rates of thermal photons emitted from a QGP and a hot hadronic gas at a given temperature are nearly identical. Compton and annihilation processes [Eqs. (2) and (3)] in the quark matter and a fairly exhaustive array of hadronic reactions involving π, ρ, ω, and η, along with the decay of vector mesons were considered.

One may argue though that the hadronic reactions included in the hadronic matter in [23, 24] are not quite exhaustive and that the inclusion of additional reactions may alter this finding. Thus the consequences of including the A_1 resonance have been discussed by authors of Refs. [47, 48], and the authors of Ref. [24] have argued that the inclusion of strange mesons may not alter this near equality.

At the same time, it is also true that the calculations reported in [23] did not include higher-order terms in α_s for the QGP part. We take the point of view that the basic result of the equality of the two rates remains ap-

proximately valid and is a very useful first approximation for identifying the p_T window where we have to concentrate for the signature of a QGP.

Thus we approximate the emission rate for both the hadronic matter and the quark matter as [23]

$$E\frac{dR}{d^3p} = \frac{5}{9}\frac{\alpha\alpha_s}{2\pi^2}T^2 e^{-u^\mu p_\mu/T}\ln\left(\frac{2.912}{g^2}\frac{u_\mu p^\mu}{T}\right), \quad (54)$$

where we have taken $g^2 = 5$, and [49] the strong-coupling constant is given by

$$\alpha_s = \frac{6\pi}{(33-2N_f)\ln(\kappa T/T_C)}, \quad (55)$$

$$\kappa = 8. \quad (56)$$

This rate of emission for photons is convoluted with the space-time history of the plasma to yield

$$\frac{dN}{d^2p_T dy} = \int\left\{\left(\frac{E\,dR}{d^3p}\right)_{\rm QGP}\Theta(\epsilon-\epsilon_Q) + \left[\left(\frac{E\,dR}{d^3p}\right)_{\rm QGP}\frac{\epsilon-\epsilon_H}{\epsilon_Q-\epsilon_H} + \left(\frac{E\,dR}{d^3p}\right)_H\frac{\epsilon_Q-\epsilon}{\epsilon_Q-\epsilon_H}\right]\Theta(\epsilon_Q-\epsilon)\Theta(\epsilon-\epsilon_H) + \left(\frac{E\,dR}{d^3p}\right)_H\Theta(\epsilon_H-\epsilon)\right\}\tau\,d\tau r\,dr\,d\eta\,d\phi. \quad (57)$$

In the following we shall add the contributions of the QGP phase and the QGP part of the mixed phase and call it emissions from quark matter (QM). Similarly, the sum of the emissions from the hadronic phase and the hadronic part of the mixed phase is called the emissions from the hadronic matter (HM). These integrations were performed using Monte Carlo techniques.

The number of photons emitted in central collisions of two lead nuclei, with and without transverse flow, at SPS, RHIC, and LHC energies is displayed in Figs. 16–18.

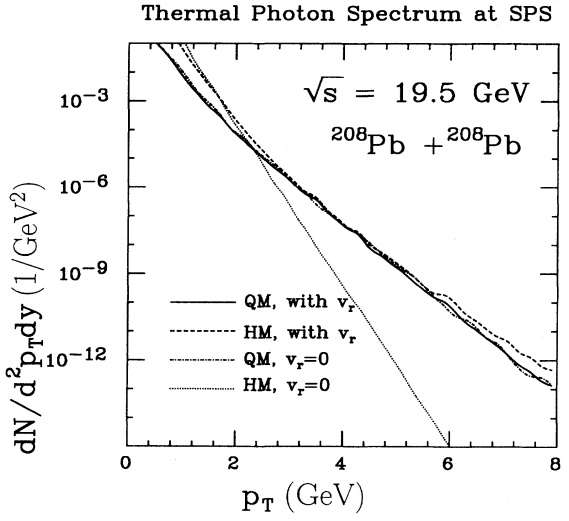

FIG. 16. Spectrum of thermal photons emitted from an expanding QGP up to the time of freeze-out, at SPS energies with and without transverse flow. The initial conditions correspond to those of Fig. 7. The solid curve gives the contribution of the quark matter (the QGP phase + QGP part of the mixed phase) with the transverse flow. Similarly the long-dashed curve gives the contribution of the hadronic matter (the hadronic part of the mixed phase + the hadronic phase) with the transverse flow. The contributions of the quark matter (short-dashed curve) and the hadronic matter (dotted curve) without the transverse flow are also given.

At SPS energies we see that emission from quark matter is essentially unaffected by the transverse flow, and *if* the transverse-flow effects are ignored, the photons from the quark matter outshine those from the hadronic matter beyond $p_T \approx 2$ GeV in conformity with the results of [20, 21, 24]. However, when the transverse-flow effects are included, the transverse kick imparted to the photons from the hadronic matter causes a complete closure of the window. No region is found where the contribution from the quark matter may outshine the contributions from the hadronic matter.

At RHIC energies, we see again that the contributions from the quark matter are not affected by the transverse expansion. However, the huge transverse kick received by the photons from the hadronic matter again makes them comparable to those from a quark-gluon plasma for p_T between 2 and 5 GeV. With the conditions envisaged here no region is found where the photons from quark matter

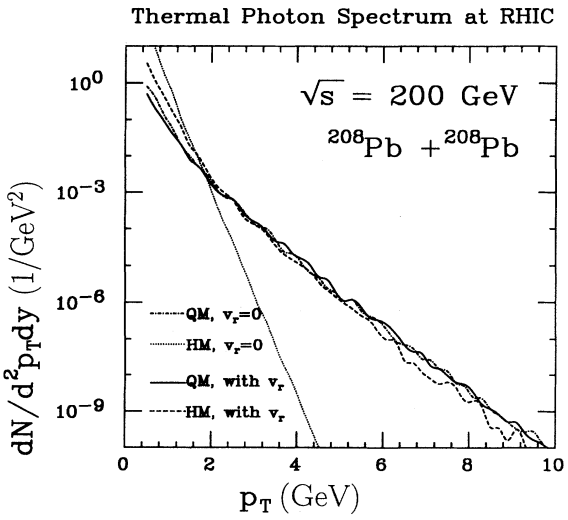

FIG. 17. Same as Fig. 16 for RHIC energies.

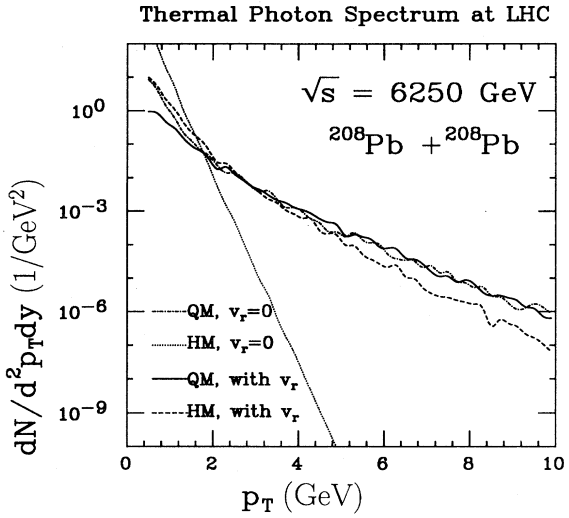

FIG. 18. Same as Fig. 16 for LHC energies.

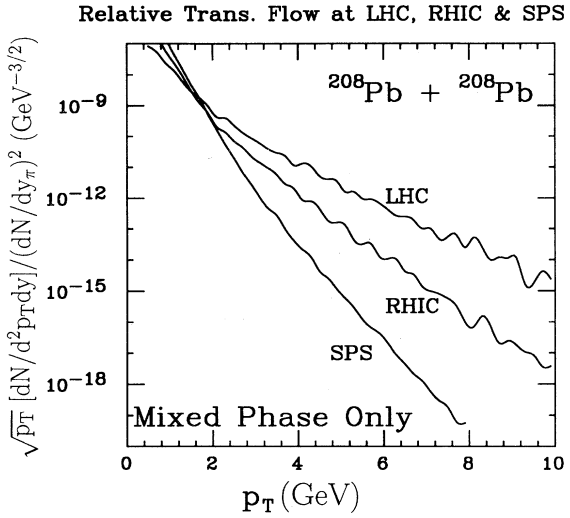

FIG. 19. Number of photons thermally emitted from the *mixed phase only,* normalized to the square of pion rapidity density and multiplied by $p_T^{1/2}$. In the absence of transverse flow the three curves at SPS, RHIC, and LHC energies would have identical slopes given by $1/T_C$. The apparent transition temperatures are 217 MeV, 273 MeV, and 417 MeV, respectively, corresponding to the average transverse flow velocities of $0.30c$, $0.49c$, and $0.74c$.

dominate over those from the hadronic matter.

At LHC energies, however, the situation is very promising. Now even the contribution from the quark matter is slightly affected by the transverse flow. Even though the transverse kick received by the photons from the hadronic matter is substantial, photons having a p_T more than 4 GeV preferentially have their origin in the quark matter.

Considering that in less optimistic conditions initial temperatures attained by the plasma may be lower, we feel that a method to delineate the transverse kick received by the photons from the hadronic matter would be very welcome.

In this context the results of Kapusta, Lichard, and Seibert [23] can be used with a great advantage. It can be easily seen that if we neglect the slow variation of the logarithmic term in Eq. (54) and also the transverse-flow effects, the contributions from the mixed phase [20, 21] would be given by

$$\frac{dN}{d^2p_T dy} \propto \left(\frac{dN}{dy_\pi}\right)^2 \frac{\exp(-p_T/T_C)}{p_T^{1/2}}. \tag{58}$$

Thus the emission of photons normalized to the square of pion multiplicity density is determined by the transition temperature T_C alone *if there is no transverse flow of the plasma.* The Doppler-shifted transition temperature due to the transverse flow is then seen to be

$$T_C^{\rm eff} = \left[\frac{1+\langle v_r\rangle}{1-\langle v_r\rangle}\right]^{1/2} T_C, \tag{59}$$

where $\langle v_r\rangle$ is some average transverse flow of the fluid during the mixed phase.

In Fig. 19 we show the result of such an exercise by plotting the number of photons emitted from the mixed phase, normalized to the square of the pion rapidity density and multiplied by $p_T^{1/2}$, for SPS, RHIC, and LHC energies. The consequences of the transverse flow are seen easily, as in its absence the three curves would have an identical slope corresponding to $1/T_C$. The effective transition temperatures thus obtained are plotted in Fig. 20. They are seen to increase almost linearly with the particle rapidity density.

Now the task of estimating the "transverse kick" may proceed in the following manner. First we note that, because of the smaller temperature and rapidly decreasing density, the contribution of the hadronic phase would be

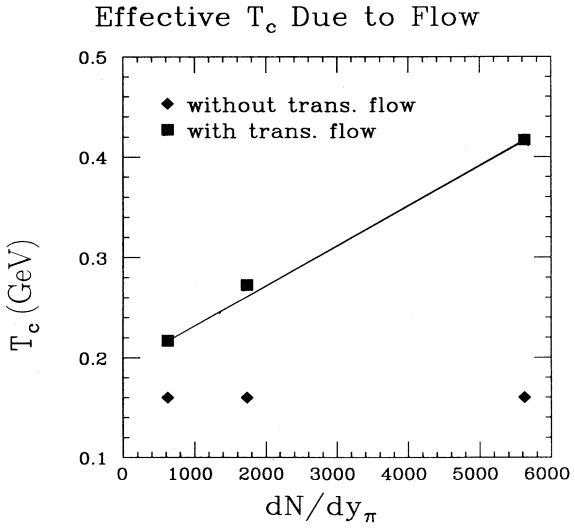

FIG. 20. Variation of the effective transition temperature due to the transverse flow at SPS, RHIC, and LHC.

small at least at very large p_T as compared to the contributions from the mixed phase and so we neglect it in the first approximation. Now we note that the sum of all the contributions, when plotted against p_T, would show a change of slope at higher transverse momenta. This is most easily seen by adding the QM and the HM contributions at the LHC energies in Fig. 18. (This change of slope would perhaps not be easily discernible at SPS and RHIC energies due to the transverse flow.) We could then associate the slope at smaller p_T with the contribution of the mixed phase which had a "known" temperature T_C which is Doppler shifted. It could also be possible to check on the Doppler shift estimated by looking at the momentum distribution of hadrons produced in the plasma [50] if we know T_C or to estimate the transition temperature T_C if we use the information about the extent of the Doppler shift. In any case, once the extent of the transverse kick for the contributions from the mixed phase is estimated, we can make corrections for it. This will immediately ensure that the contribution of the QGP phase stand out very smartly.

In Fig. 21 we show the change in the average transverse momentum of the photons due to the transverse flow. Only photons having $p_T > 500$ MeV have been included. We see that while in the absence of the transverse flow the average transverse momentum of the photons is nearly constant, it increases by almost 40% at LHC, by about 12% at RHIC, and only by 5% at SPS. In this sense we feel that the results from SPS, RHIC, and LHC may compliment each other.

In this context it may also be possible to disentangle [51] the extent of transverse flow by looking at the ratio of $\gamma/\mu^+\mu^-$ as a function of the invaraint mass M of the dileptons, for different p_T. This aspect has its origin in the fact that dileptons having different invariant masses suffer different amount of transverse flow.

We complete this discussion by noting that the average transverse-flow velocities $\langle v_r \rangle$ at SPS, RHIC, and LHC energies for the mixed phase in the scenario envisaged here are 0.296, 0.488, and 0.743, respectively.

It is interesting to note that the authors of Ref. [50] obtain a value of about 0.40–0.45 for $\langle v_r \rangle$ from the analysis of hadron spectra at SPS energies. We should remember though that the transverse velocity estimated here is some kind of average over the space-time history of the plasma up to the end of mixed phase, whereas that of [50] gives it essentially at the time of freeze-out.

In any case it should be worthwhile to develop a scheme to unfold the effect of transverse expansion on the photon spectrum. In this connection we may add that Srivastava and Kapusta [52] have recently explored the utility of photon interferometry to understand the history of the evolution of quark-gluon plasma. The Bose-Einstein correlation function for two photons has been shown to single out regions of space and time over which the collective flow velocity is not large. This may help us to identify photons having their origin in the quark-gluon plasma.

It should be remembered that hydrodynamic calculations give an upper limit on the extent of the transverse flow. Thus a value of the freeze-out temperature other than 100 MeV taken in all the calculations reported above may alter our conclusion about the p_T windows in a significant manner. In order to test this, we have plotted the results for RHIC energies by taking the freeze-out temperatures as 80, 100, 120, 140, and 160 MeV, respectively (Fig. 22). We note that the results are quite sensitive to the freeze-out temperature used, and if a higher freeze-out temperature is taken, a clear p_T window is seen to emerge where the QGP photons dominate over those from the hadronic matter. The freeze-out temperature can in principle be obtained by comparing the dimensions of the system with the mean free path of the hadronic matter consisting of π, ρ, ω, and η. The sensitivity of the results on the freeze-out temperature can perhaps be eliminated by adding a contribution of free-

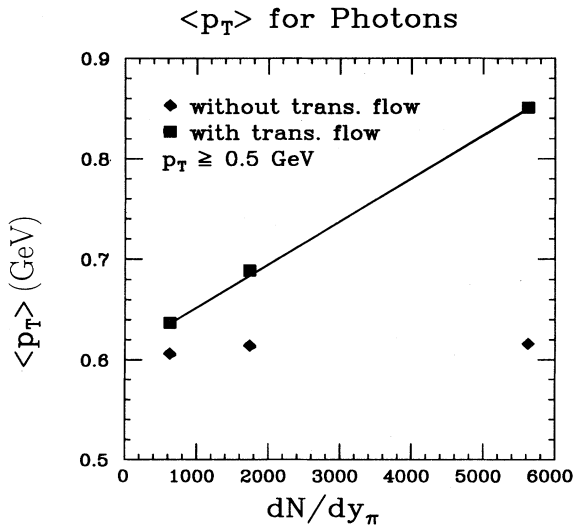

FIG. 21. Average transverse momentum of thermal photons having ($p_T > 500$ MeV) due to transverse flow.

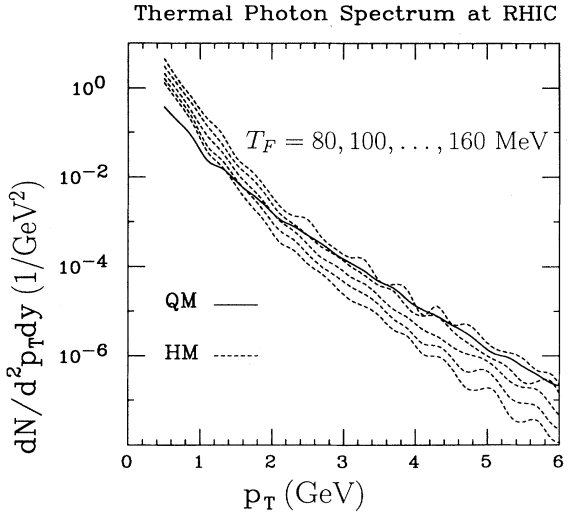

FIG. 22. Sensitivity of hadronic matter contributions to the freeze-out temperature at RHIC energies, for thermal photons.

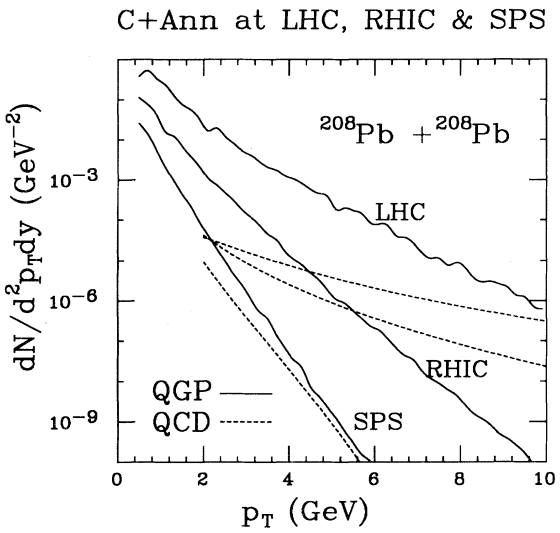

FIG. 23. Number of photons thermally emitted from the *QGP phase only,* and the direct QCD photons due to Compton and annihilation processes at SPS, RHIC, and LHC. Note that at LHC energies the bremsstrahlung contribution is large (Fig. 6).

streaming gas [27] of hadrons after the freeze-out [53].

It is also felt that it may be more reasonable to treat at least the latter stages of the hadronic phase, which impart the largest transverse kick, as a hadronic cascade [54]. This will considerably minimize the transverse kick received by the photons.

Finally, in Fig. 23 we show our results for thermal photons from the QGP phase and the QCD photons at SPS, RHIC, and LHC energies due to the Compton and annihilation processes. This illustrates the challenge of identifying the photons having their origin in the QGP over and above the QCD photons. We assume the ideal situation when the decay photons from π^0 and η after the freeze-out have been singled out by an invariant-mass analysis [25]. We also assume that the photons during and after the advent of the mixed phase have been singled out by noting the slope at smaller p_T as discussed above.

V. SUMMARY

The feasibility of using photons to study the dynamic evolution of quark-gluon plasma likely to be created at SPS, RHIC, and LHC energies, in collisions involving two lead nuclei, has been studied. The transverse-flow effects are shown to be quite large for emissions from the mixed phase and from hadronic phase and negligible for the QGP phase. The extent of the transverse kick was estimated by assigning an apparent temperature to the mixed phase. This was found to be about 220 MeV at SPS energies, 270 MeV at RHIC energies, and a phenomenal 490 MeV at LHC energies when the "true" transition temperature is 160 MeV.

At LHC energies, photons having $p_T > 4$–5 GeV are shown to have their origin predominantly in the QGP phase. At SPS and RHIC energies, no such window is found because of the transverse flow. It is suggested that one may be able to delineate the transverse-flow effects for the mixed phase by noting the change of slope in the spectrum of photons in going from a smaller to larger p_T, which would be very welcome indeed. The location of the p_T window is shown to be very sensitive to the value of the freeze-out temperature assumed. It is also felt that as most of the transverse kick is accumulated during the last stages of the collision, where the hydrodynamics may not be strictly valid, the results given here may be taken as the upper limit of the transverse flow. If instead the latter stages of the hadronic phase are described by a combination of a hadron cascade and a free-streaming gas of hadrons, the sensitivity of the results to the freeze-out temperatures may be minimized. This will also lead to relatively smaller transverse flow than seen here.

The photons from direct QCD processes have been evaluated, and it is shown that perturbative QCD can be used with reasonable confidence to evaluate this background at larger p_T. The fragmentation of a final-state quark in parton-parton scattering leading to a photon is shown to be the largest QCD background at LHC.

ACKNOWLEDGMENTS

One of us (D.K.S.) is grateful to J. Kapusta and L. McLerran for many useful discussions and for their critical comments on the manuscript. Our special thanks are to K. Kajantie, M. Kataja, and V. Ruuskanen for a useful correspondence and for making the transverse expansion code available to us. D. K. Srivastava's research at the University of Minnesota was supported by the U.S. Department of Energy under Grant No. DOE/DE-FG02-87ER40238.

[1] L. McLerran, Rev. Mod. Phys. **58**, 1021 (1986), for a good overall perspective of the field.
[2] L. van Hove, Z. Phys. C **27**, 135 (1985).
[3] M. Gyulassy, K. Kajantie, H. Kurki-Suonio, and L. McLerran, Nucl. Phys. **B237**, 477 (1984).
[4] L. P. Csernai and J. Kapusta, Phys. Rev. Lett. **69**, 737 (1992); Phys. Rev. D **46**, 1379 (1992).
[5] Bo Nilsson-Almqvist and E. Stenlund, Comput. Phys. Commun. **43**, 387 (1987); K. Werner and P. Koch, Phys. Lett. B **242**, 251 (1990).
[6] X.-N. Wang and M. Gyulassy, Phys. Rev. D **44**, 3501 (1991).
[7] T. Matsui and H. Satz, Phys. Lett. B **178**, 416 (1986).
[8] J. A. Lopez, J. C. Parikh, and P. J. Siemens, Phys. Rev. Lett. **53**, 1216 (1984).
[9] J. Rafelski, Phys. Lett. B **262**, 333 (1991).
[10] L. Feinberg, Nuovo Cimento A **34**, 39 (1976).
[11] E. Shuryak, Phys. Lett. **78B**, 150 (1978).

[12] F. Halzen and H. C. Liu, Phys. Rev. D **25**, 1842 (1982).
[13] B. Sinha, Phys. Lett. **128B**, 91 (1983).
[14] L. McLerran and T. Toimela, Phys. Rev. D **31**, 545 (1985).
[15] R. C. Hwa and K. Kajantie, Phys. Rev. D **32**, 1109 (1985).
[16] K. Kajantie, J. Kapusta, L. McLerran, and A. Mekjian, Phys. Rev. D **34**, 2746 (1986).
[17] M. Neubert, Z. Phys. C **42**, 231 (1989).
[18] D. K. Srivastava and B. Sinha, Phys. Lett. B **261**, 1 (1991).
[19] S. Raha and B. Sinha, Int. J. Mod. Phys. A **6**, 517 (1991).
[20] D. K. Srivastava, B. Sinha, M. Gyulassy, and X.-N. Wang, Phys. Lett. B **276**, 285 (1992).
[21] D. K. Srivastava and B. Sinha, J. Phys. G **18**, 1467 (1992).
[22] K. Kajantie, M. Kataja, L. McLerran, and P. V. Ruuskanen, Phys. Rev. D **34**, 2153 (1987).
[23] J. Kapusta, P. Lichard, and D. Seibert, Phys. Rev. D **44**, 2774 (1991).
[24] S. Chakrabarty, J. Alam, D. K. Srivastava, B. Sinha, and S. Raha, Phys. Rev. D **46**, 3802 (1992).
[25] H. Gutbrod (private communication).
[26] U. Heinz, P. Koch, and B. Friman, in *Proceedings of the ECFA Large Hadron Collider Workshop,* Aachen, Germany, 1990, edited by G. Jarlskog and D. Rein (CERN Report No. 90-10, Geneva, Switzerland, 1990), Vol. II, p. 1079.
[27] J. Kapusta, L. McLerran, and D. K. Srivastava, Phys. Lett. B **283**, 145 (1992).
[28] K. Geiger, Phys. Rev. D **46**, 4965 (1992); **46**, 4896 (1992).
[29] P. V. Ruuskanen, in *Quark Matter '91*, Proceedings of the 9th International Conference on Ultrarelativistic Nucleus-Nucleus Collisions, Gatlinburg, Tennessee, 1991, edited by T. C. Awes *et al.* [Nucl. Phys. **A544**, 169c (1992)].
[30] T. Ferbel and W. R. Molzon, Rev. Mod. Phys. **56**, 181 (1984).
[31] J. F. Owens, Rev. Mod. Phys. **59**, 465 (1987).
[32] M. Fritz and P. Minkowski, Phys. Lett. **69B**, 316 (1977).
[33] F. Halzen and D. M. Scott, Phys. Rev. D **18**, 3378 (1978).
[34] R. Rückl, S. J. Brodsky, and J. F. Gunion, Phys. Rev. D **18**, 2469 (1978).
[35] P. Aurenche, A. Douiri, R. Baier, M. Fontannaz, and D. Schiff, Phys. Lett. **140B**, 87 (1984).
[36] R. Gandhi, F. Halzen, and F. Herzog, Phys. Lett. **152B**, 261 (1984).
[37] G. Anassontriz *et al.*, Z. Phys. C **13**, 277 (1982).
[38] D. W. Duke and J. F. Owens, Phys. Rev. D **22**, 2280 (1984).
[39] J. Badier *et al.*, Z. Phys. C **31**, 341 (1986).
[40] C. De Marzo *et al.*, Phys. Rev. D **36**, 8 (1987).
[41] J. D. Bjorken, Phys. Rev. D **27**, 140 (1983).
[42] H. von Gersdorff, M. Kataja, L. McLerran, and P. V. Ruuskanen, Phys. Rev. D **34**, 794 (1986).
[43] B. Friman, K. Kajantie, and P. V. Ruuskanen, Nucl. Phys. **B266**, 468 (1986).
[44] A. Bialas, W. Czyz, and A. Kolawa, Acta Phys. Pol. B **15**, 229 (1984).
[45] E. V. Shuryak, *The QCD Vacuum, Hadrons and the Superdense Matter* (World Scientific, Singapore, 1988), pp. 323.
[46] J. P. Boris and D. L. Book, J. Comput. Phys. **11**, 38 (1973).
[47] L. Xiong, E. Shuryak, and G. E. Brown, Phys. Rev. D **46**, 3798 (1992).
[48] C. S. Song, Phys. Rev. C **47**, 2861 (1993).
[49] F. Karsch, Z. Phys. C **38**, 147 (1988).
[50] K. S. Lee, U. Heinz, and E. Schnedermann, Z. Phys. C **48**, 525 (1990).
[51] J. Alam and B. Sinha (unpublished).
[52] D. K. Srivastava and J. Kapusta, Phys. Lett. B (to be published); "History of Quark Gluon Plasma Evolution from Photon Interferometry," University of Minnesota Report No. TPI-MINN/14-T (unpublished).
[53] D. K. Srivastava and J. Kapusta, Phys. Rev. C **48**, 385 (1993).
[54] G. Bertsch, M. Gong, L. McLerran, P. V. Ruuskanen, and E. Sarkkinen, Phys. Rev. D **37**, 1202 (1988).